Metals and Materials International
https://doi.org/10.1007/s12540-024-01696-8

Phenomenological Model for the Dynamic Superplastic Deformation Mechanism in a Zn-Al Eutectoid Alloy Modified with 2 wt% Cu

Mitsuo Ramos Azpeitia[1] · E. Elizabeth Martínez Flores[1,2] · Antonio Alberto Torres Castillo[2] · Jose Luis Hernandez Rivera[3] · Gabriel Torres Villaseñor[4]

Received: 30 January 2024 / Accepted: 6 April 2024

Abstract
In this work, superplastic behavior in tension for the Zn-21Al-2Cu alloy was reviewed as a function of: grain size, temperature and strain rate. The deformation mechanism was studied under conditions where the greatest elongation was reached, characterizing microstructural changes and analyzing the associated mechanical response such as the study of plastic stability. This analysis allowed us to propose a phenomenological model consisting of five steps for the mechanism of superplastic deformation under which dynamic conditions are involved for this alloy. In the first stage, an accommodation of the microstructure was observed, in the second stage sliding by individual grain boundaries (GBS) was activated, which provided the conditions for stationary plastic flow. In the third stage, GBS was hampered by the tendency of grain boundaries remaining from high temperature phase (FβBs) to align at 45°. This fact caused the onset of plastic instability. The fourth stage consisted of a transition in which there was competition between individual and cooperative GBS mechanisms, which increased plastic instability. In the last stage, the FβBs were aligned parallel to tensile direction, which favored the GBS, and an additional diffusion flow mechanism allowed partial recovery of stable plastic flow.

Keywords Superplasticity · Deformation mechanism · Zn-Al-Cu alloys

1 Introduction

The phenomenon that produces plastic elongations greater than 200% in metals and alloys is called superplasticity [1–3]. Although this phenomenon has been observed in several alloys, the Zn-22Al eutectoid alloy is one of the most studied under different microstructural conditions and using different techniques [4–7]. In this alloy maximum engineering strains values close to 3000% along with a flow stress of 10 MPa have been reported in specimens deformed at 503 K and 10^{-2} s^{-1} [4–7]. Initial microstructure of this alloy does not exhibit significant changes caused by the large deformations [8, 9] and as a consequence, plastic flow remains homogeneous up to deformations of approximately 700%–800% [10]. These observations allowed Langdon to propose that, for this alloy, the deformation process takes place entirely under conditions that allow steady creep [11]. This proposal implies that a single mechanism of Grain Boundary Sliding (GBS) acts preferentially during the entire deformation process. Although the GBS is the most accepted deformation mechanism, there is experimental evidence that shows that this mechanism could be modified or assisted by another one [3, 12].

The Zn-21Al-2Cu alloy is a modified Zn-Al eutectoid alloy with Cu to improve its formability and mechanical properties. In a previous work it was reported that the Zn-21Al-2Cu alloy could be deformed in tension under superplastic conditions at 513 K and 10^{-3} s^{-1}, achieving engineering strains of about 1000% [13]. In this alloy, superplastic deformation remained stable only up to 50% of

✉ Mitsuo Ramos Azpeitia
mitsuo.ramos@uaslp.mx

[1] Facultad de Ingeniería-U.A.S.L.P. Dr. Manuel Nava 8, Zona Universitaria, San Luis Potosí Z.C 78290, Mexico

[2] Instituto de Metalurgia- Universidad Autónoma de San Luis Potosí, Sierra Leona 550, Lomas 2a Sección, San Luis Potosí 78210, Mexico

[3] CONAHCYT-Instituto de Metalurgia- Universidad Autónoma de San Luis Potosí, Sierra Leona 550, Lomas 2a Sección, San Luis Potosí 78210, Mexico

[4] Instituto de Investigaciones en Materiales-U.N.A.M, P.O BOX 70-360, México, D.F. México Z.C 04519, Mexico

Published online: 30 May 2024

engineering strain ($\varepsilon = 0.4$) and it was quasi-stable up to 100% ($\varepsilon = 0.7$), while for larger strains, deformation became highly localized in the central area of specimen [14]. When analyzing the microstructure of this alloy, it was observed that when deformation begins, a microstructure composed of equiaxial and fine grains prevailed, resulting in homogeneous plastic flow [15]. However, with increasing strain ($\varepsilon > 0.7$), microstructure exhibited changes such as grain growth, flow banding, and movement of residual grain boundaries originating from the high-temperature phase. These alterations inhibited that homogeneous plastic deformation further progressed [15]. For Zn-21Al-2Cu alloy, the onset of plastic instability and changes in microstructure observed for deformations greater than 50% of engineering strain, evidenced that GBS mechanism (which promotes homogeneous superplastic flow) prevails only in the initial stage of deformation process ($\varepsilon < 0.4$). This observation suggests that for values greater than 50% of engineering strain ($\varepsilon > 0.4$), the addition of 2 wt% Cu modifies the mechanism that controls plastic strain in the eutectoid alloy (Zn-22Al).

Superplasticity can be considered as a particular case of the creep phenomenon and it is associated with three mechanisms that occur at atomic level. These mechanisms are intergranular dislocation slip, grain boundary sliding, and diffusional flow [2]. In some cases, a mechanism may be necessary to allow the accommodation of other when plastic deformation occurs at high temperature [12]. It is necessary to show the specific details of how each one of these mechanisms acts and the interrelationships that are developed between them during superplastic flow. This information can be obtained by observing the macro and micro structural changes occurring during deformation. All the previously mentioned mechanisms are thermally activated and controlled by diffusion, therefore, constitutive relationships for the study of superplasticity are same as those described for creep. Most important feature in high temperature creep mechanism is that strain rate (ε) varies with stress (σ), temperature (T) and grain size (d) according to Dorn's Eqs. [1, 2, 3]:

$$\dot{\epsilon} = \left(\frac{ADGb}{kT}\right)\left(\frac{b}{d}\right)^{p}\left(\frac{\sigma}{G}\right)^{n} \tag{1}$$

where D is the diffusion coefficient ($= D_o \exp -Q/RT$), k is the Boltzman's constant, n is the stress exponent ($n = 1/m$), G is the shear modulus, b is the Burguers vector, p represents the exponent of the sensitivity to grain size, σ is the flow stress and A is a constant that is dependent of the microstructure. Each creep mechanism can be described by this equation and the specific values assignated to the parameters n, p and D. Calculating these values is essential for determining the mechanism that promotes the steady-state deformation occurrence.

The fact that in several superplastic alloys have been observed that no appreciable changes occurs in the original microstructure formed by equiaxed grains, has led to propose GBS mechanism as the main deformation mode during the superplastic deformation process [1, 16]. GBS is a deformation mode that involves relative grains displacement along surface of their common boundary. For GBS to occur, an accommodation process is necessary to maintain contact between grains [16–18]. This accommodation process is an important part of the deformation mechanism and includes microstructural rearrangements such as grain boundary migration, grain rotation, grain emergence and dislocation motion [19–21]. It can be considered that the accommodation process is the main stage controlling the complete deformation mechanism [18].

Although GBS is the most widely accepted mechanism to describe superplastic deformation, the use of advanced characterization techniques has made it possible to demonstrate additional microstructural changes, such as grain elongation and element segregation [22–24], which can be recognized as GBS modifications or an additional mechanism that acts during the superplastic deformation process [25]. In addition, the GBS mechanism promotes the achievement of steady flow conditions, which remain constant with increasing strain and result in a homogeneous plastic flow. However, in some alloys, particularly at large strains, instabilities have been reported in the homogenous plastic flow [14, 26] which are associated with fluctuations in the strain rate sensitivity parameter (m) as a consequence of so me microstructural changes occurring during deformation [2]. Therefore, a strong correlation exist between microstructural changes and instability plastic flow, which has been used to propose that in these alloys, the initial deformation mechanism undergoes significant modifications as a function of the strain increments.

The main objective of this work is to propose a phenomenological model for the dynamic superplastic deformation mechanism in the Zn-Al eutectoid alloy modified with 2 wt% Cu considering conditions of grain size, temperature, and strain rate where the highest elongation is achieved. This model is based on new experimental evidence obtained for this alloy in addition to previous results obtained from superplastic deformation tests in tension [13], the values calculated to evaluate the plastic instability process [14] as well as the observed microstructural changes resulting from superplastic deformation [15]. This work represent the culmination of these preliminary systematic research.

2 Materials and Methods

The fabrication details of the Zn-21Al-2Cu alloy sheets are described in a previous work [13]. Tensile testing specimens with a gauge length (Lo) of 6.35 mm were machined from these sheets. They were subjected to a heat treatment that consisted of the following steps: solubilization at 623 K for 1 h followed by quenching in water at 288 K, subsequent annealing at 533 K for durations ranging from 0.5 h to 90 h to obtain a microstructure of fine grains with an average grain size between 0.85 μm and 4.5 μm. The grain size measurements were performed using the intercept method after a conventional metallographic preparation of specimens using diamond paste for polishing step with a 3 and 1 μm in size.

To evaluate the superplastic behavior of the Zn-21Al-2Cu alloy, tensile tests were carried out at constant crosshead speed until fracture occurred by using a universal testing machine equipped with a thermal chamber. The temperature and strain rate conditions for the tests varied from 413 K to 513 K and from 10^{-3} s^{-1} to 10^{-1} s^{-1}, respectively. Microstructural changes on surface of deformed specimens were characterized by Scanning Electron Microscopy (SEM) and energy dispersive X-ray energy dispersive spectroscopy (EDS). Mappings for the elements Zn, Al and Cu were performed on images taken at 35,000 magnification using a JEOL model JSM-6610LV SEM. The plastic instability evaluation, determination of the strain rate sensitity index (m) and the strain-hardening (γ) coefficient as a function of the strain increments, were carried out as described in previous work [14].

3 Experimental Results

3.1 Initial Microstructure Features

After the quenching treatment and subsequent annealing to stabilize grain size of the Zn-21Al-2Cu alloy, a fine mixture of phases rich in Zn and Al was obtained from the transformation of the high-temperature beta phase. Due to the Zn content, the transformation that occurred was β (triclinic) → η phase (hcp) + R (rhombohedral), as described for the eutectoid alloy of the Zn-Al system [27]. Where R is a transition phase that transforms into the mixture of phases: η (hcp) + α (fcc), which are phases rich in Zn and Al, respectively.

The size and shape of the final microstructure will depend on the quenching rate, as well as the temperature and time used during the solubilization and annealing process. In Fig. 1, microstructures are shown after homogenization using two different annealing times at 533 K. In both cases, microstructure consists of fine grains of η and α surrounded by residual grain boundaries of the high-temperature β phase indicated with letter A in Fig. 1a, and 1b. These residual boundaries divide the microstructure into equiaxed groups or domains. β residual boundaries seem to be formed mainly by α-phase aligned grains, however it is important to note that these domains are incomplete in most cases, i.e., boundaries of β-phase grains are not fully conserved.

It has been suggested that this phase distribution in the Zn-22Al-2Cu alloy is probably due to small deviations from eutectoid composition caused by addition of 2 wt%. Cu, which promoted the presence of proeutectoid α phase around residual boundaries coming from the high temperature β phase [28]. Due to the similarity with the microstructural arrangements reported by other authors for Zn-22Al alloy [29], in this work residual boundaries will be called Former Beta Boundaries (FβBs). A close inspection of the Fig. 1 shows that most of FβBs are composed of continuous sections of aligned α phase and discontinuous sections formed by fine grains of α and η phases. Because of superplastic deformation, it is expected that FβB tend to break. This behavior probably turns these FβBs fragments into obstacles that hinder and delay sliding of fine grains when deformation increases.

3.2 Tensile Deformation Behavior

Tensile behavior of Zn-21Al-2Cu alloy was evaluated as a function of the initial grain size, temperature, and strain rate. Figure 2 shows the engineering stress-strain curves for the tensile tests that were conducted. In each individual test depicted in Fig. 2, a similar behavior was observed during

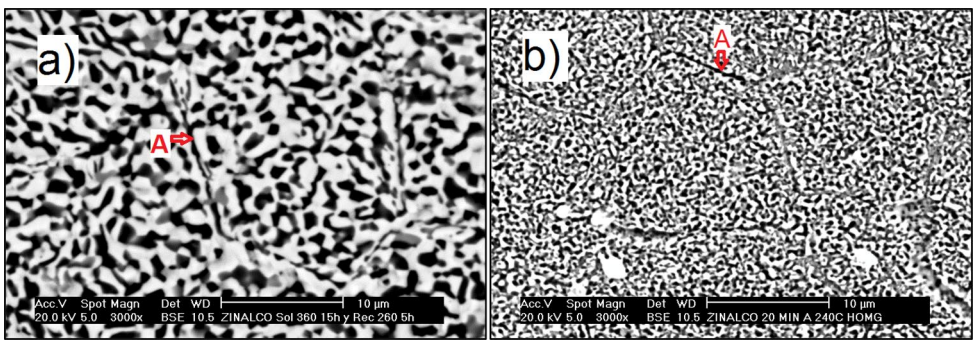

Fig. 1 Variation of the Zn-21Al-2Cu alloy microstructure using two annealing conditions after a solution and quenching treatment. In both cases, a mixture of α and η phases was observed, enclosed by residual boundaries of the high-temperature β phase (indicated by the letter A in micrographs). (**a**) Annealing for 5 h at 533 K, (**b**) Annealing for 20 min at 533 K

the tensile tests, which was characterized by a constant increase in stress until reaching a maximum, followed by a decrease in stress until reaching a practically constant value on this parameter as strain was increased.

Based on these results, it was observed that the maximum plastic deformation, which was close to 1000%, was obtained for samples with an initial grain size of 0.85 μm deformed at a strain rate of 10^{-3} s^{-1} and a temperature of 513 K. Images of samples deformed under different conditions are also shown in Fig. 2. The presence of an inhomogeneous plastic flow that tends to stabilize in final part of the deformation process was observed.

Results of the grain size effect at 513 K and temperature effect for a grain size of 0.85 μm on the flow stress and on the total plastic deformation capacity at a strain rate of 10^{-3} s^{-1} are observed in Fig. 3a, b, respectively. Under these conditions, flow stress increased as the grain size increased and decreased as temperature increased too. The amount of

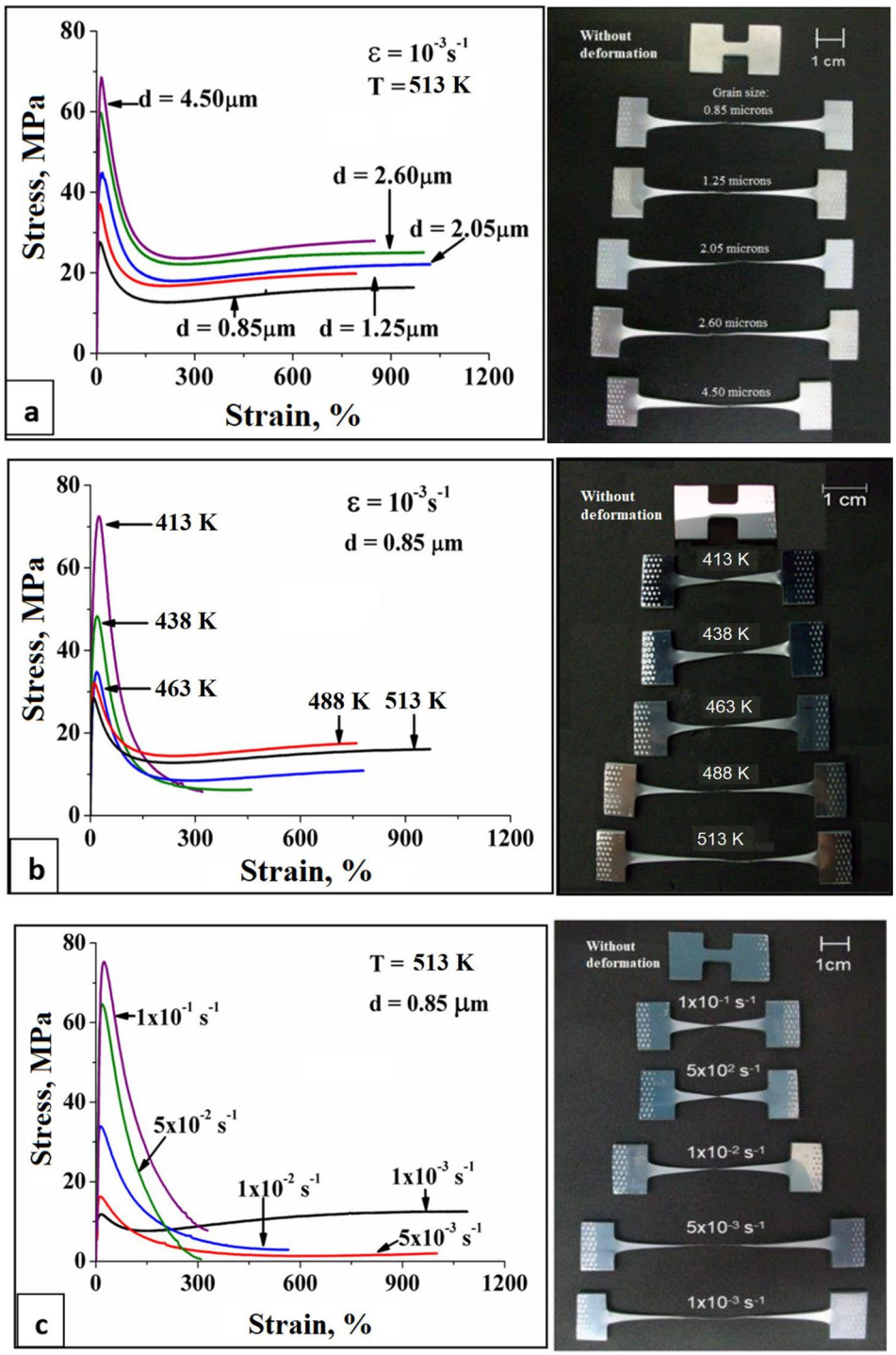

Fig. 2 Engineering stress-strain curves and Zn-21Al-2Cu alloy deformed specimens as a function of: (**a**) Grain size, (**b**)Temperature and (**c**) Strain rate

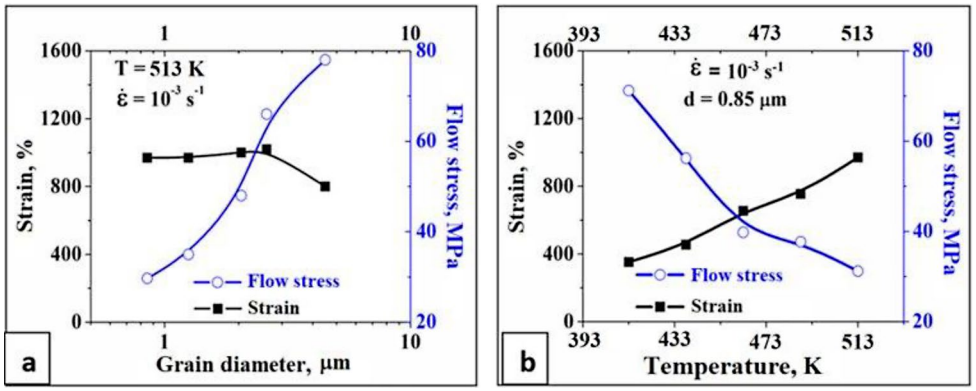

Fig. 3 Flow stress and deformation capacity for Zn-21Al-2Cu alloy as a function of: (**a**) Initial grain size and (**b**) Test temperature

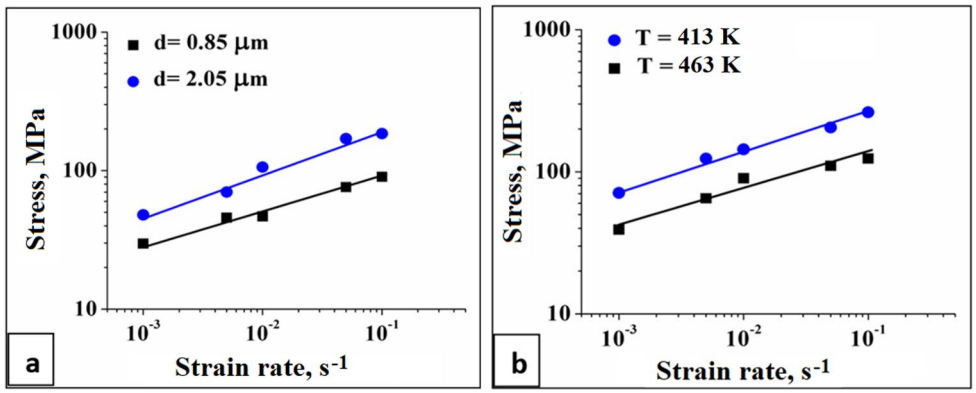

Fig. 4 Flow stress for Zn-21Al-2Cu alloy as a function of strain rate. (**a**) For two grain sizes, (**b**) For two temperatures

plastic deformation is only affected when grain size is larger than 2 μm and it increased as temperature also increased. The fact that the flow stress decreased with temperature indicates that deformation process was thermally activated, and therefore, an activation energy can be associated with this process.

Stress as a function of strain rate was studied by varying the sample grain size at 513 K, and in another set of experiments by varying temperature for samples with a grain size of 0.85 μm; the results are shown in Fig. 4a, b, respectively. In both cases, the stress value increased with the increments in the strain rate. The value of the strain rate sensitivity index (m) can be calculated from the slope of the curves. The m values calculated were 0.3 and 0.24, for grain sizes of 2.05 and 0.85 μm, respectively; and 0.29 and 0.24 for temperatures of 413 and 463 K, respectively. In all cases, the values of m are lower than those reported for the Zn-22Al alloy deformed under similar conditions, where the m values varied between 0.45 and 0.55 [30, 31]. For the Zn-21Al-2Cu alloy, it was observed that the growth of m value is directly proportional to the grain size and inversely proportional to the temperature. This suggests that the presence of 2 wt% Cu modified the dependence of the value of m on grain size and temperature.

The m values for the Zn-21Al-2Cu alloy suggest a quasi-superplastic behavior as plastic flow is not homogeneous throughout the complete deformation process. This characteristic was observed for all deformed specimens as a function of grain size, temperature and strain rate, where the total deformation is composed of a homogeneous initial deformation, which in all cases is less than 100%, followed by non-homogeneous deformation that can reach up to 900%. This contrasts with the observations reported for Zn-22Al, where plastic flow remains homogeneous up to values of 800% [10]. The differences in the deformation capacity between the two alloys are related to variations in the m values. These suggest that presence of 2 wt%. Cu causes a real decrease in m parameter that leads to early plastic instability. This instability results in a smaller amount of homogeneous deformation and, consequently, a decrease in the total deformation.

3.3 Instability of the Plastic Flow

In a previous work, the plastic flow instability of Zn-21Al-2Cu alloy was evaluated under optimal conditions to induce a superplastic behavior (strain rate of 10^{-3} s^{-1} and 513 K). The findings indicated that by adding 2 wt% Cu to the Zn-22Al eutectoid system, the stable superplastic deformation capacity of this alloy decreased approximately from 700 to 100% [14]. It was determined that in the Zn-21Al-2Cu alloy plastic deformation remains quasi stable only up to 100% ($\varepsilon = 0.7$), beyond which deformation becomes highly localized for larger strains. The onset of plastic instability, which

was determined by the Hart and Wilkinson-Cáceres criteria, occurs at ε = 0.4 [14]. This observation aligns with the low initial values of both, strain-rate sensitivity (m) and strain-hardening coefficient (γ), which tend to decrease as a function of true strain, as can be observed in Fig. 5a, b. These values were calculated using the metodology described in a previuos work [14].

The onset of this plastic instability provides evidence that GBS mechanism, which allows steady-state superplastic flow, was dominant only in the first stage of the deformation process for Zn-21Al-2Cu alloy. Decrements in values of m and γ parameters may be related to the microstructural changes ocurring during deformation. These changes are associated with strain-induced grain growth in the fine α and η phases, which produced effective strain hardening and increased with strain. The quantitative contribution of strain to grain growth for Zn-21Al-2Cu alloy was previously evaluated [14]. It was observed that the presence of 2 wt% Cu doubled the strain-induced grain growth rate compared to that observed for eutectoid Zn-22Al alloy doped with 0.5 wt% Cu. Furthermore, this grain growth predominantly ocurred in the Zn-rich phase [14].

Grain size growth during superplastic deformation has been reported for different alloys [20, 32]. It has been proposed that this phenomenon has both a static contribution (assisted by diffusion) and a dynamic contribution (assisted by deformation) [20, 33]. Wilkinson and Cáceres found that growth exhibited a linear dependence with respect to deformation [32, 34]. Figure 6a shows the static and dynamic contributions to grain growth in Zn-21Al-2Cu alloy. It was observed that both contributions, increased linearly with deformation and the greatest contribution corresponded to dynamic growth assisted by deformation process. Sato and Kuribayashi proposed that to assessing this contribution requires considering, the effect of diffusive processes [20]. Figure 6b compares the dynamic contribution to grain growth in the Zn-21Al-2Cu and Zn-22Al alloys, considering the Sato and Kuribayashi criterion, for which, grain growth is given by $Ln(d_D/d_s)$, where d_D represents grain growth due to deformation and d_s is the growth due to heating [20].

Results in Fig. 6b show that the dynamic contribution to grain growth was higher for the Zn-21Al-2Cu alloy than for the Zn-22Al alloy. This suggests that the addition of copper facilitated the mechanism by which dynamic grain growth occured. Sato and Kuribayashi proposed that strain-assisted growth can be expressed by the equation [20]:

$$\frac{\partial_D}{\partial \varepsilon} = \alpha d \tag{2}$$

where α, is a constant with an approximate value of 0.3 for various biphasic alloys [20]. For Zn-21Al-2Cu alloy, the value of this constant was approximately 0.6 and was calculated from the corresponding line slope in the graph shown in Fig. 6b. This value was closer to that predicted with Wilkinson and Cáceres model for grain growth in two-phase alloys [34]. In this model, growth occurrs when two grains of same phase come into contact and coalesce. This type of growth mechanism is favored because the diffusion rate at grain boundaries is accelerated by an increasing concentration of vacancies caused by the deformation process. This fact facilitates migration of grain boundaries, which in turn favors grain growth [19, 35].

Finally, Table 1 summarizes the principal features observed during the evaluation of the superplastic behavior in Zn-21Al-2Cu alloy. This table includes the characteristics reported for the Zn-22Al alloy for comparison purposes. The data presented in this table indicate that the presence of Cu does not affect the dependence of superplastic behavior on the grain size, temperature and deformation rate. However, the presence of Cu decreases the maximum strain capacity, increases the flow stress and affects the plastic stability, by decreasing the value of the parameter m. From the evidence presented in this investigation, the role pricipal of the Cu addition in the Zn-22Al alloy is to decrease the m and γ parameters as a consequence of microstructural changes during deformation. These changes involved the deformation-induced grain growth in the α and η fine phases as well as other microstructal modifications suchs as the movement of the FβBs.

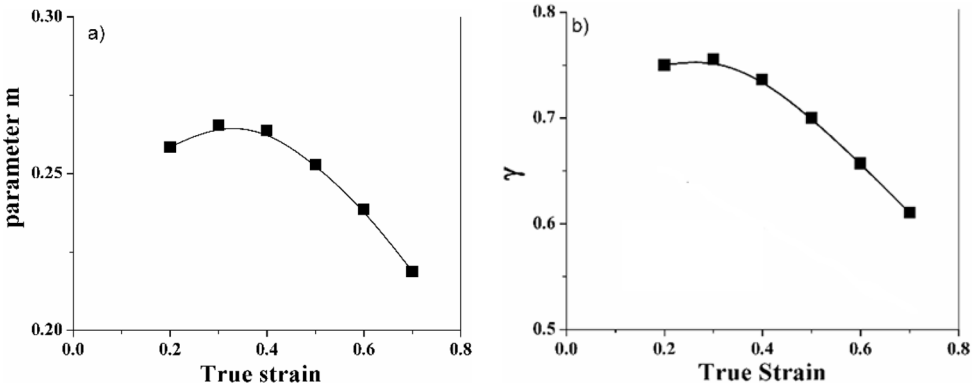

Fig. 5 (**a**) Estimation of strain-rate sensitivity index m and (**b**) Strain-hardening coefficient γ as function of true strain for Zn-21Al-2Cu alloy

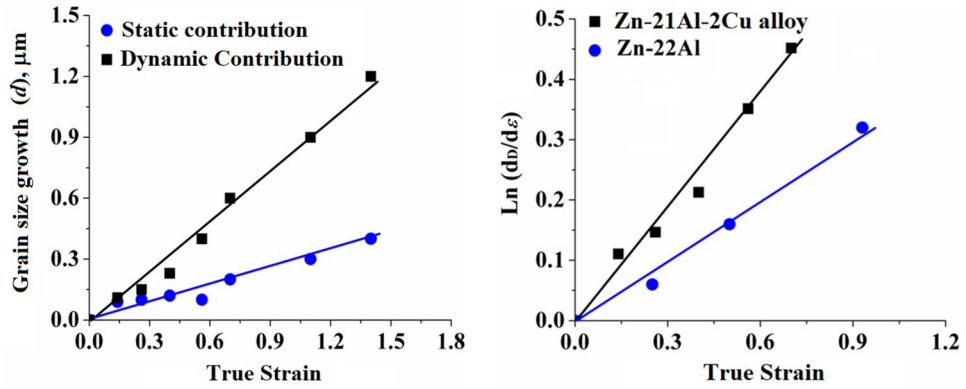

Fig. 6 (**a**) Static and dynamic contributions to grain growth of Zn-21Al-2Cu alloy as strain function. (**b**) Dynamic contribution to grain growth for the alloys Zn-21Al-2Cu and Zn-22Al as a function of strain, considering the Sato and Kuribayashi criteria

Table 1 Principal features of the superplastc behavior of the Zn-21Al-2u alloy and Zn-22Al alloy

Feature	Zn-21Al-2Cu alloy (this study)	Zn-22Al alloy
Máximum deformation capacity	1000% in optimal conditions.	2800% in optimal conditions.
Flow stress interval	25–180 Mpa in the strain rate interval evaluated (5×10^{-4} s^{-1}– 1 s^{-1}).	3–80 Mpa in the strain rate interval evaluated (5×10^{-4} s^{-1}– 1 s^{-1}).
Relationship between flow stress and strain rate	Lineal in the strain rate interval evaluated (5×10–4 s-1–1 s-1).	Lineal in the strain rate interval evaluated (5×10^{-4} s^{-1}– 1 s^{-1}).
m value	0.25–0.29	0.45–0.55
Grain size effect	With an increase in grain size, there is a corresponding increase in flow stress. However, the impact on deformation capacity remains minimal.	An increase in grain size leads to a rise in flow stress, while simultaneously reducing the capacity for deformation.
Temperature effect	As the temperature increases, the flow stress decreases and increase in deformation capacity.	As the temperature increases, the flow stress decreases and increase in deformation capacity.
Strain rate effect	An increase in the strain rate leads to a rise in flow stress, while simultaneously diminishing the capacity for deformation.	An increase in the strain rate leads to a rise in flow stress, while simultaneosusly diminishing the capacity for deformation.
Stability of the plastic flow	Under optimal conditions it remains stable up to deformations less than 100% and then decreases suddenly with increasing deformation.	Under optimal conditions it remains stable up to deformations of 800%, gradually decreasing with deformation.
Activation energy Q value	72.7–77.7 kJ/mol	67–80 kJ/mol

3.4 Dorn Equation Parameters as Function of Strain

In a previous work, it was determined that for the Zn-22Al-2Cu alloy the value of parameter m is low (m ≈ 0.26) and that it decreased as function of true strain, so there were no conditions to maintain a stable plastic flow [14]. If it is considered that m = 1/n, changes in parameter m as a function of strain, must generate changes in the value of parameter n. This fact also suggests that other parameters of the Dorn equation should also change when strain increases. The values of parameter p for this alloy were also determined previously, constructing graphs of log σ versus log d for different strain values, using data corresponding to tensile tests carried out at 10^{-3} s^{-1} and 513 K with an initial grain size of 0.85, 2.05 and 4.5 µm [14]. Results confirmed that parameter p tended to decrease with increasing strain after reaching a maximum value of 2.18 for a true strain of 0.2 [14]. For a superplastic 7075Al alloy, a similar behavior was reported for m and p values as a function of true strain, and this changes were related to microstructural changes [36].

Activation energy (Q) is an important parameter of superplastic flow because it reflects the nature of thermally activated processes that control the strain rate. The Q magnitude is usually determined by tests carried out at constant stress or at constant strain rate within a certain range of temperature. The Q value for the Zn-21Al-2Cu alloy was calculated in a previos work under the same conditions used in this study and its value ranged between 72.7 and 77.7 kJ/mol, with an average of 75.1 ± 2.45 kJ/mol [13]. This average value is within the range of values reported for the Zn-22Al alloy, which range between 67 and 80 kJ/mol [12, 31, 37]. The average value of Q for Zn-21Al-2Cu alloy, is in the level of activation energy necessary for diffusion through grain boundaries in pure Zn (60 kJ/mol) and in pure Al (69 kJ/mol). This indicates that under steady flow conditions, the GBS mechanism is favored. By other hand the value of Q as a function of strain (see Fig. 7) was estimated using Eq. 3 and the values of n determined in a previous work [13].

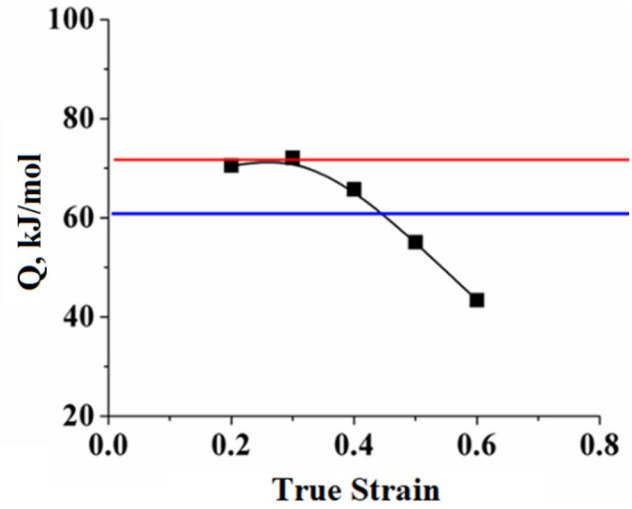

Fig. 7 Activation energy parameter Q stimation in the Zn-22Al-2Cu alloy as a function of the true strain

$$\frac{\sigma^n}{TG^{n-1}} = A'' \exp\left(Q/RT\right) \tag{3}$$

As can be seen in Fig. 7, that the value of Q decreased for true strains values greater than 0.3. The horizontal lines in the graph indicate the activation energy values that favor diffusive processes through the grain boundary in Al (upper line) and in Zn (lower line). Analysis of these results indicated that, for true strains greater than 0.45, the deformation mechanism assisted by diffusive processes through the grain boundary became difficult. This critical value agreed well with the values at which the onset of creep instability was observed. The tendency of the Q value to continue decreasing as true strain increased, suggested that the GBS mechanism was difficult to occur.

3.5 Microstructural Evolution

In a previous work, evolution of the microstructure in samples of the Zn-21Al-2Cu alloy, deformed as a function of strain rate and temperature, was reported [15]. It was observed that with a true strain of 0.15 (see Fig. 8a), the FβBs tended to break because of the individual movements of the phases α and η by grain boundary sliding (GBS) mechanism specifically in specimens deformed under conditions where the greatest elongation was achieved (10^{-3} s^{-1} and 513 K). In Fig. 8a it can be observed evidence of the formation of new surfaces due to diffusional mass transport. These regions were result of the operation of a GBS mechanism assisted by diffusion.

For larger strains, ε = 1.4, the microstructure showed changes in regions with the highest plastic deformation. Equiaxed α phase and η phase grains formed elongated regions that were aligned in tensile direction (see Fig. 8b). The α phase presented changes in its shape and size, which indicated that a diffusion mechanism occurred and promoted grain growth. This mechanism was favored by the deformation process. On the other hand, the η phase elongation could be assisted by the redistribution of elements by diffusion, as proposed in a previous work [15]. Other researchers have reported and discussed similar microstructural changes as evidence of modification in the main mechanism of superplastic deformation for samples of the Zn-Al eutectoid alloy, with large amounts of strain in tension [38].

Microstructural characterization results on surface of the Zn-21Al-2Cu alloy specimens deformed in tension showed that η phase had a greater deformation capacity compared to α phase. As was mentioned before, this increment in deformation capacity may be related to a redistribution of elements favored by deformation-assisted diffusive processes. For the Zn-21Al-2Cu alloy, this redistribution can be favored preferentially in η phase than in α phase if the homologous deformation temperature of each phase (T_H) is taken into account, where T_H=Td/Tm (Td is deformation

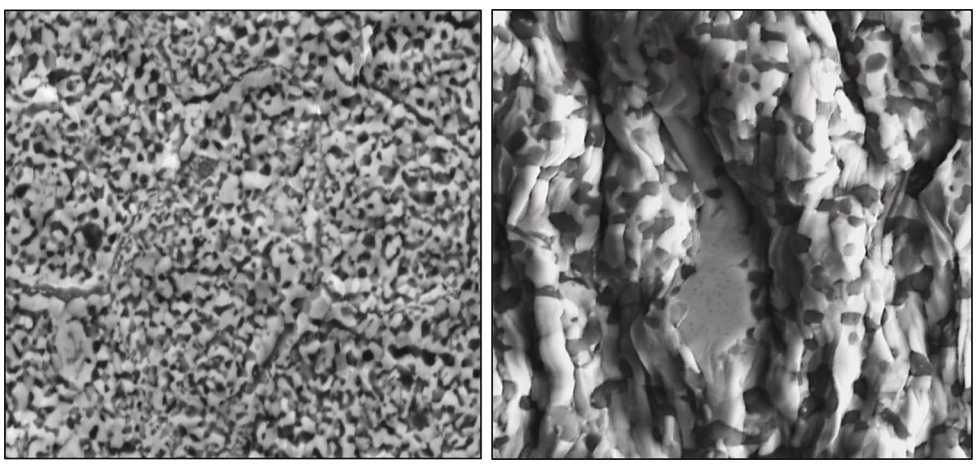

Fig. 8 Microstructures of Zn-21Al-2Cu alloy at 5,000X corresponding to different true strain in a tensile specimen deformed at a strain rate of 10^{-3} s^{-1} and 513 K. (**a**) ε = 0.15, (**b**) ε = 1.4

temperature and Tm is melting temperature, both in Kelvin). For Zn-21Al-2Cu alloy, at a temperature of 513 K where the greatest deformation was observed, the homologous temperature was 0.74 for η phase, while it was 0.55 for α phase. These differences can generate conditions that favor a more significant redistribution of elements in η phase in comparison to α phase.

In order to investigate whether the redistribution of elements was promoted in phases presents in Zn-21Al-2Cu alloy during superplastic deformation, EDS maps showing the distribution of Zn, Al and Cu were obtained. Figures 9 and 10 show respectively EDS maps for the microstructure of a sample before deformation and for a specimen deformed at 513 K and 10^{-3} s^{-1}. These EDS maps only provide a qualitative approximation of elements distribution, since the characteristic X-ray signal, given the voltage used, may come from an interaction volume that is larger than the phases.

Figure 9a shows that microstructure of the sample before deformation was formed by equiaxed α phase grains with a size less than 1 μm, which were surrounded by interconnected regions of η phase. In this micrograph, it can also be observed a grain of the τ' phase that had an stoichiometry of Al_4Cu_3Zn (gray grain in the center). The EDS maps for distribution of Zn (red), Al (blue) and Cu (green) corresponding to this microstructure are presented in Fig. 9b–d, respectively. In these EDS maps, the outline of some grains was drawn to easily distinguish the distribution of each element (Zn, Al and Cu) within each phase (α, η and τ′). As expected, it was observed that most of Zn was within the η phase and most of Al was within α phase. This distribution was in accordance with the equilibrium stoichiometry of the α and η phases, which are solid solutions rich in Al and Zn, respectively. In the EDS map of Fig. 9d, it can be seen that most of the Cu was located in the τ′ phase and only a minor amount was distributed in the α and η phases.

Figure 10a shows a micrograph corresponding to a deformed area. This figure shows presence of flow bands described in a previous section of this work. Micrograph shows some α phase grains with a size of approximately 1 μm and what appear to be elongated η-phase grains with a width of 1 μm and a length greater than 3 μm. EDS maps in Fig. 10b–d show, the distribution of elements Zn, Al and Cu for the α and η phases, respectively. These maps show that α phase was enriched in Al and η phase was enriched in Zn. It was also observed that Cu continued distributed in

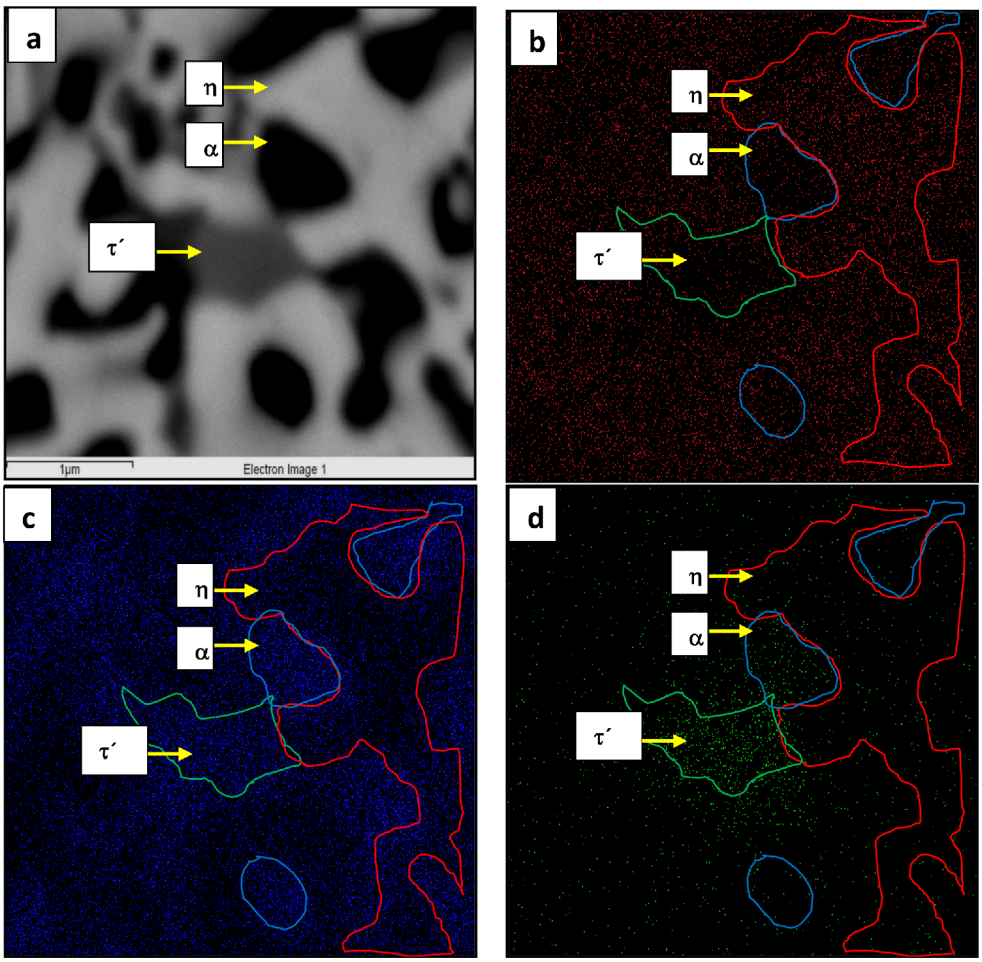

Fig. 9 (**a**) SEM micrograph at 35,000X showing microstructure on the surface of Zn-21Al-2Cu alloy sample before deformation and EDS maps showing distribution of (**b**) Zn, (**c**) Al and (**d**) Cu

both phases. These results suggested that there was a redistribution of Al and Zn between the α and η phases because deformation process took place at high temperature. Results also suggested that Zn was the element that diffused most easily. It was expected if it was taken into account that the diffusion coefficient of Zn, with a value of 1.8×10^{-3} m^2/s, is greater than that of Al, whose value is 2.25×10^{-4} m^2/s. It was observed that the Zn contained in α phase migrated to η phase, leaving the α and η phases enriched in Al and Zn, respectively.

Changes observed in the elements distribution of EDS maps in Fig. 10, suggested that there was a significant diffusion of these elements between the phases. This matter transport was also reported by Kaibyshev et al. in Zn-22Al alloy where the Zn-rich phase tended to bealigned in the tensile direction [39]. On the surface of the superplastically deformed Zn-21Al-2Cu alloy samples, an enrichment of Zn in the η phase and of Al in α phase was observed as a consequence of deformation. These findings allowed us to propose that η phase grains on surface were enriched with Zn, through a mass transport mechanism favored by a strain-assisted diffusion process. This enrichment promoted that grains of this phase had a composition close to that of pure Zn, as shown in Fig. 10b. Under these conditions, a deformation mechanism assisted by the slip of planes can be favored, resulting in their large deformation capacity observed. Ths is opposite with the α phase where the enriched in Al and Cu enhanced mechanical properties of this phase.

4 Discussion

4.1 Phenomenological Model

Langdon proposed that, for eutectoid Zn-22Al alloy, in which an approximate maximum of 2800% engineering strain was reached at 523 K, the deformation process was carried out under conditions that allow constant creep, therefore it was believed that a single mechanism acted during deformation process [11]. Initial microstructure of this alloy, formed by fine grains, did not present significant changes during deformation [8, 9], so plastic flow remained homogeneous up to deformations of approximately 800%

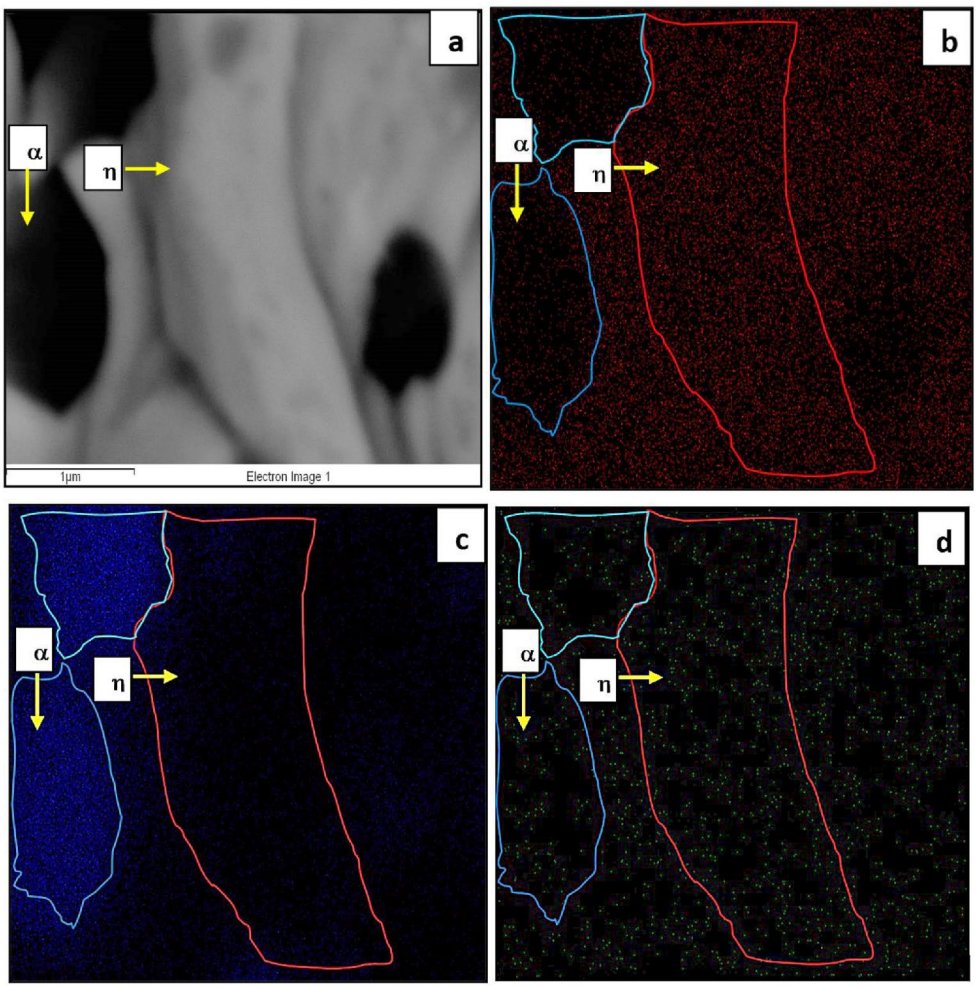

Fig. 10 (**a**) SEM micrograph at 35,000X showing flow bands in microstructure on the surface of Zn-21Al-2Cu alloy sample after deformation at 513 K and 10^{-3} s^{-1} and EDS maps showing distribution of (**b**) Zn, (**c**) Al and (**d**) Cu

[10]. On the other hand, when 2% by weight of Cu was added to Zn-22Al alloy, it was possible to obtain a maximum elongation of approximately 1000%, when deformation was carried out under conditions like those used for Zn-22Al alloy [13]. Characterization of the Zn-21Al-2Cu alloy deformed specimens showed that for this alloy there were changes, both at microstructural and macrostructural level, which were a function of the increments in the deformation. These changes indicated that the plastic flow did not remain stable throughout the entire deformation process but rather changed as deformation was increased.

Therefore, the model that describes the deformation mechanism for Zn-21Al-2Cu alloy should consider the observed microstructural and macrostructural changes. In this work, a phenomenological model is proposed considering both, the observations of microstructural evolution and results of the analysis of plastic stability process. The model is proposed for Zn-21Al-2Cu alloy specimens deformed in uniaxial tension with a strain rate of $10^{-3}s^{-1}$ at 513 K, conditions under which the greatest elongation was observed. The obtained results allowed us to describe the deformation process of this alloy, dividing it into five stages based on the increments in true strain. These stages are described in detail below.

Stage 1 (ε = 0.0–0.2) In the elastic region, grains move providing conditions for a steady-state plastic flow.

Figure 11a shows the microstructure of a specimen deformed up to ε = 0.15. It is observed that in this first stage of deformation both, the fine grains of α phase and the interconnected regions of η phase moved. Movement of the grains of both phases broke the coherence between grain boundaries and allowed their equiaxed shape to be distinguished. This movement also caused the FβBs to emerge, forming a relief that allowed them to be distinguished. This was also due to the movement of the α and η phases.

The evolution of a microstructure in which equiaxed grains are not distinguished towards one in which they are perfectly defined occurred in the elastic region (ε = 0.0–0.2). In this stage the aspect ratio of grains is stabilized; the applied stress is enough to move grains without causing plastic deformation. This caused an increment in misorientation angles indicating the loss of coherence between grain boundaries, which in later stages will facilitate GBS. It has been reported that strain value at which an equiaxed microstructure is reached, is a function of the nature and thermomechanical history of the alloy, as well as the temperature and strain rate used during deformation process [40]. For the Zn-21Al-2Cu alloy, the true strain values ranged between 0.15 and 0.25 depending on the grain size, temperature, and strain rate. Under the conditions considered for the proposed phenomenological model (d = 1 μm, 513 K and strain rate of 10^{-3} s^{-1}), the first stage was defined in the elastic region of the material, for a true deformation values up to 0.20, which corresponded to the value at which flow stress was determined for this alloy.

It is proposed that during this first stage, the operative mechanisms are the accommodative processes that promote the rearrangement and adjustment of grains, creating conditions to facilitate GBS. Sato and Kuribayashi have suggested that if a microstructure does not have the characteristics for superplastic deformation, then deformation at a specific temperature and strain rate can activate the dislocation network, modifying the grain boundary structure [20]. Based on this idea, it is thought that in this first stage, the stress and temperature will favor the grains movement because the dislocations present at grain boundaries are activated (mainly in η phase). The grain boundary migration, assisted by diffusion creep, also contributes to GBS between individual grains, which was evidenced by the relief produced by FβBs when they emerged to the surface and by the formation of new surfaces (letter A in Fig. 11a).

The evolution of the microstructure towards more equiaxed one, allowed us to propose that in Zn-21Al-2Cu alloy the dislocations tended to move towards the grain boundaries in a similar way to what occurs in a dynamic polygonization process reported for a superplastic Al-Mg-Mn alloy [41]. This process promoted the formation of straighter boundaries, which facilitates the GBS process

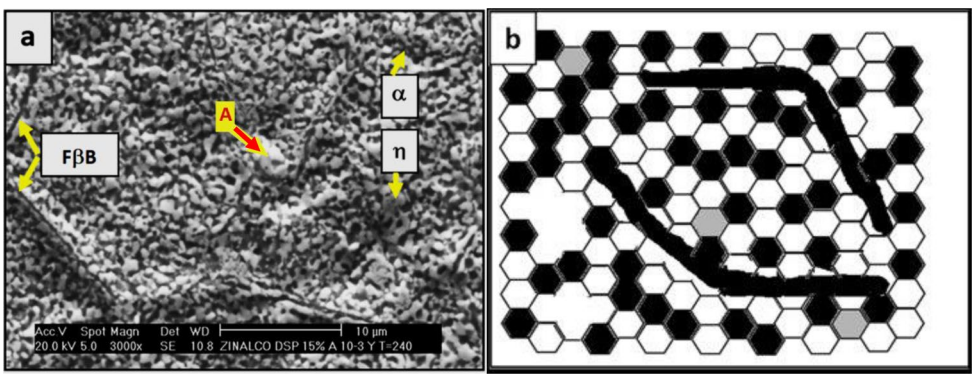

Fig. 11 (**a**) Micrograph showing microstructure for a true strain 0.15 in a tension sample of Zn-21Al-2Cu alloy. (**b**) Scheme for the first stage of the model

because there was more contact between the neighboring grain boundaries of the different phases. This first stage of deformation mechanism is schematized in Fig. 11b.

Stage 2 (ε = 0.2–0.4) Individual grains slide through a GBS mechanism, producing a steady-state plastic flow.

For this stage, no significant changes in microstructure of equiaxed grains were observed after a true strain of 0.4 (see Fig. 12a), indicating that the main mechanism for deformation was the individual GBS, in which strains values of 60%–90% were achieved as reported for the Zn-22Al alloy [9]. To assist this mechanism, it was necessary to maintain the accommodation process described above with increasing strain. At this stage, additional microstructural features, such as grain rotation, grains emerging from interior to the surface, and deformation-assisted grain growth, were observed and considered as part of the GBS accommodation process.

Grains must rotate during deformation to facilitate the grain boundary sliding. In a previous work, it was shown that the distribution of misorientation angles of grain boundaries changed due to superplastic deformation process, evidencing the rotation of α and η grains in the Zn-21Al-2Cu alloy [42]. Furthermore, the microstructure after a true strain of 0.4 showed evidence of new grains emerging towards the sample surface, as shown in results obtained from the surface analysis of a deformed sample by using atomic force microscopy (AFM) [15]. This process, which must occur to fill the gaps that are generated due to the movement of grains, also contributes to maintaining the stability of the microstructure [19].

The proposed model also considers that in this second stage some of the FβBs fragment and move due to deformation. This is schematized in Fig. 12b, which represents the microstructural changes described above. The scheme shows some grains emerging from the inner layers (letter A), migration of grain boundaries (letter C) as well as rotation (letter B) and growth of some grains (letter D). It is considered that all these are factors facilitate microstructure accommodation. It is important to note that FβBs (letter A in Fig. 12a), serve as guides so that fine grains of α and η phases are adjacent to them and also are aligned with them. The accommodation process described above occurs as strain increases to favor the individual GBS mechanism, which allows the maintenance of steady plastic flow conditions.

It is proposed that this mechanism continues acting until changes in the FβBs and accommodation processes (grain rotation, grain boundary migration, grain size growth and grain emergence) promote the third stage of deformation process, in which plastic instability begins.

Stage 3 (ε = 0.4–0.7) Microstructural changes lead to transition stage which result in the onset of plastic instability.

In this stage, which begins with a true strain of 0.4, it was observed that the GBS became more difficult, because there were debris of the FβBs that were not aligned with the tensile axis, making grain sliding around these zones difficult. The observed behavior for true strain value at this stage agreed with decrease in activation energy for the GBS mechanism, calculated previously and shown in Fig. 7. The Fig. 13a shows the microstructure of a sample that was subjected to a true strain of 0.69. It is observed that grains of α and η phases that surround a fragment of a FβB, are oriented at 45 º (letter B in Fig. 13a), and do not seem to be aligned with the tensile axis (dotted lines). Additionally, grain size of both phases in this area is lower (letter A in Fig. 13a), which indicates that the accumulation of stresses limited material diffusion and made it difficult the movement of fine grains.

The stress concentration can be relieved, either by the generation of intragranular dislocations that form subgranular boundaries or by the fragmentation of some FβBs. The partial formation of new grains has been reported for several superplastic alloys and it has been described as a dynamic recrystallization process that occurs through the continuous nucleation of dislocations [43]. In Fig. 13a, it is also observed that there were areas where grains of α and η phases were aligned parallel to the axis of load application.

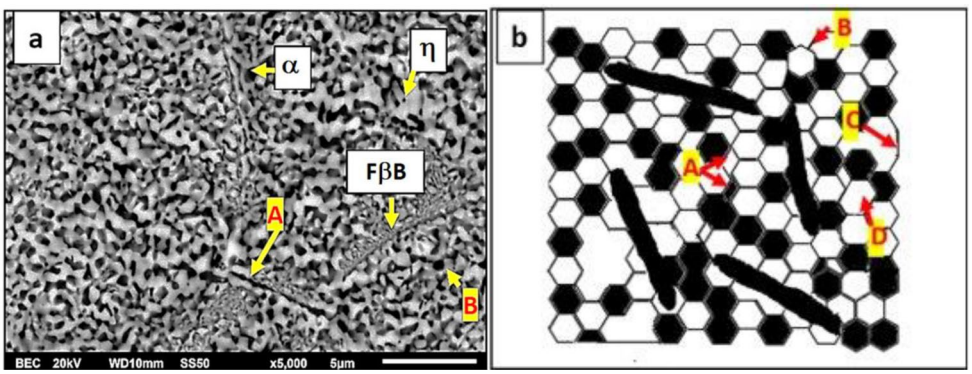

Fig. 12 (**a**) Micrograph showing microstructure for a true strain of 0.4 in a tension sample of the Zn-21Al-2Cu alloy. (**b**) Scheme for the second stage of the model

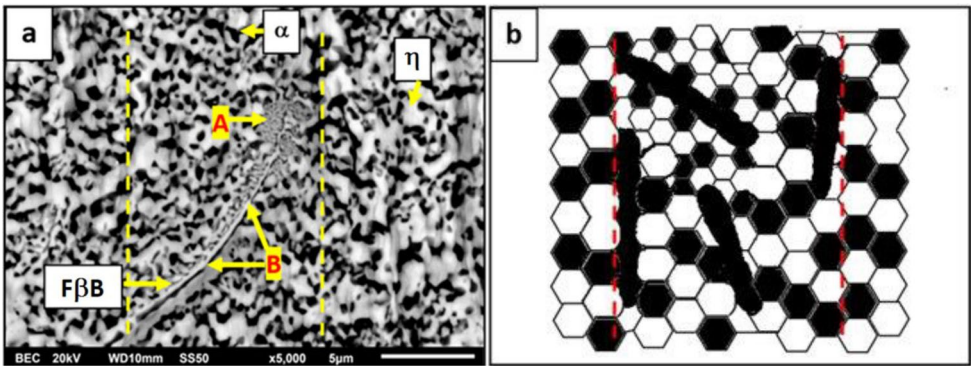

Fig. 13 (**a**) Micrograph showing microstructure for a true strain of 0.69 in a tension sample of Zn-21Al-2Cu alloy. (**b**)Scheme for the third stage of the proposed model

In these areas, a low number of FβBs were also aligned with tension axis. This alignment of FβBs, indicates the beginning of flow bands formation on the deformed samples surface, as was reported in a previous work [15].

Figure 13b shows the proposed scheme for this third stage, where the main characteristic is the presence of some residual FβBs that are not aligned with tensile axis. Their primary effect is to hinder the movement and alignment of fine grains of α and η phases. Based on the observed changes in microstructure for this stage, it is proposed that as the strain increases, some FβBs break, allowing grains of α and η phases to align with the tensile axis. However, the residual FβBs that did not align or break, block the flow of fine grains of these phases. Therefore, at this stage there are regions where the individual GBS mechanism is hindered by non-aligned FβBs and regions where the aligned FβBs serve as guides that lead the flow of fine grains in direction of the tensile axis. This situation generates a non-homogeneous stress state that promotes the beginning of plastic instability process. Finally, the FβBs that did not align with the tensile axis, will serve as guides for the collective movement of the small grains trapped around them. This movement will occur through a mechanism of cooperative grain boundary sliding (CGBS), which will be described in the fourth stage of the model.

Stage 4 (ε = 0.7–1.5) An additional CGBS mechanism competes with individual GBS, leading to an increase in plastic instability.

At this stage, some FβBs that are not aligned with the tensile axis coincide at their ends, forming barriers that delimit groups of fine grains identified with the letter A in Fig. 14a. This figure shows the microstructure corresponding to a true strain of 1.0. This causes the edges of these grains to orient themselves, increasing the coherence between them, a fact which favors cooperative movement [44]. The CGBS occurs through a process of cooperative grain boundary migration that adapts to the microstructure. In the model proposed for Zn-21Al-2Cu alloy, this migration process was promoted by the misalignment of some FβBs that joined their ends during deformation. The presence of this mechanism results in an increase in plastic instability and promotes the formation of surface reliefs described as flow bands in a previous work [15].

Some authors have stated that if a cooperative sliding mechanism is active, the formation of reliefs is expected due to the operation of cutting strips that activate the cooperative movement of grains [44, 45]. For the Zn-21Al-2Cu alloy, it is proposed that this mechanism acts up to true strain value close to 1.5. For larger deformations, the common boundary alignment process become more difficult, because non-aligned FβBs stop serving as guides when they break or align in the direction parallel to tensile axis.

In the microstructure observed in this fourth stage of the proposed model, which is schematized in Fig. 14b, some grains of the α and η grew with respect to previous stage in some areas, as indicated with letter B in Fig. 14a. This growth, which was greater for grains of η phase (indicated with letter C in Fig. 14a), is caused by dynamic growth promoted by deformation as proposed in Sect. 3.3. The greater growth of η phase grains, can be explained by the migration of aluminum dissolved in η, causing its enrichment in Zn. This fact resulted in an increase in the diffusion coefficient of Al in this phase, as can be seen in Fig. 10. Although for this stage, the main mechanism that acts is CGBS, evidence was found that the individual GBS mechanism is still operating. However, it is proposed that at this stage, this latter mechanism is used more as part of the accommodation process of the cooperative mechanism.

Stage 5 (ε > 1.5) Individual GBS and a flow by diffusion allowed a stable plastic flow to be partially recovered.

This stage of the proposed model will be observed for true strains greater than 1.5, where the most of FβBs have already been broken or aligned parallel to the tensile axis, which reduced stress concentration. This stress relaxation initially allows the grains of α and η phases to grow, as can be seen in Fig. 15a for a sample with a true strain of approximately 2.0.

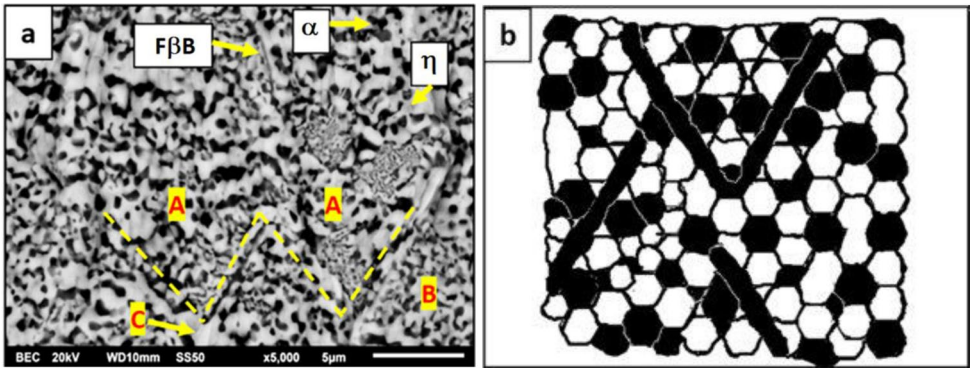

Fig. 14 (**a**) Micrograph showing microstructure for a true strain of 1.0 in a tension sample of Zn-21Al-2Cu alloy. (**b**) Scheme for the fourth stage of the proposed model

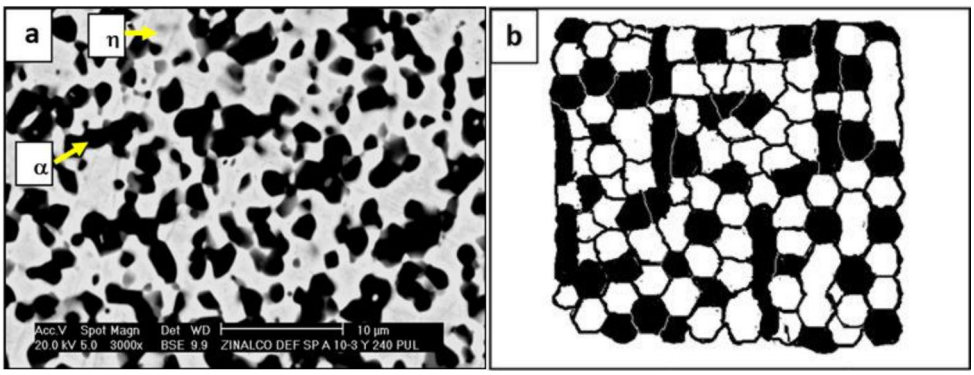

Fig. 15 (**a**) Micrograph showing microstructure of a sample of Zn-21Al-2Cu alloy with a true strain of 2.0. (**b**) Scheme for the last stage of the model

These grains will move through an individual GBS mechanism, which is made more difficult by the growth of grains. The transient recovery of this individual GBS mechanism allows the material to be deformed again through a partially stable plastic flow.

Figure.15b shows the scheme for this stage, where grains of the η phase tend to be interconnected, while α grains remain equiaxed. This microstructural feature can be expected if it is considered that α phase does not deform easily and remains equiaxed during superplastic deformation because its composition changes (see Fig. 10). It results in a composition close to a 7xxx aluminum alloy series, with a yield strength of approximately 500 MPa [46]. Therefore, the behavior of α phase grains is like that of hard particles present in a soft matrix composed of η phase, which is mainly zinc.

According to observed changes in the microstructure, it is proposed that for a large plastic deformation ($\varepsilon > 1.5$), α phase continues to deform mainly by a GBS mechanism, while η phase tends to deform mainly through a mechanism of diffusional flow. The differences between mechanisms that act and the deformation capacities for each phase, depend on their homologous temperature, defined in Sect. 3.3. For α phase the homologous temperature is 0.55 and for η phase it is 0.74. This difference between homologous temperatures explains why η phase shows a greater capacity for plastic deformation that allows it to achieve a notable elongation, which causes formation of flow bands on the surface. In contrast, α phase behaves like an elastic solid while retains its equiaxed shape. Formation of these flow bands in Zn-21Al-2Cu alloy was reported in a previous work [15]. The results agree with observations made by Motohashi and Shibata for Zn-22Al alloy; they reported that the great elongation of Zn-rich phase plays an important role in deformation mode of that alloy [38].

4.2 Dorn Equation for Proposed Model

Various mathematical equations have been developed to describe deformation mechanism in superplastic alloys, but it is always assumed that the entire deformation process takes place under steady flow conditions [9]. Therefore, for these alloys the Dorn equation is valid throughout deformation process. However, if the flow is modified as deformation increases, as described for the Zn-21Al-2Cu alloy in a previous section, then it is only possible to propose an equation that describes the deformation mechanism for stages 2 and 3 ($0.2 < \varepsilon < 0.7$) in which a stable flow was observed in this alloy.

The equation proposed for this alloy was based on the Dorn equation, which describes deformation of metallic alloys at high temperature (Eq. 1). As mentioned before, deformation mechanism is characterized by the values of critical parameters in this expression. For Zn-21Al-2Cu alloy, these parameters were calculated in a previous work [13]. Based on these results, it was established that the

equation that described the strain rate when steady-state flow conditions are reached is:

$$\dot{\varepsilon} = 1.7x10^{8}\frac{DGb}{kT}\left(\frac{b}{d}\right)^{2.5}\left(\frac{\sigma}{G}\right)^{3.9} \quad (4)$$

Equation 4 was used to determine theoretical values of flow stress as a function of strain rate for Zn-21Al-2Cu alloy, and the results are presented in Fig. 16. These theoretical values are compared with values obtained experimentally in Sect. 3.1. The experimental values agreed with data calculated using Eq. 4, confirming that for the studied strain rate range (5×10^{-4} s^{-1}– 1 s^{-1}), the mechanism that acted to achieve steady-state plastic flow conditions was the same as that observed in other alloys. According to the parameter values in Eq. 4, this mechanism was an individual GBS [11, 16]. Based on the findings from the study on plastic stability, we can confirm that this equation holds for true strain values not exceeding 0.4.

In the proposed phenomenological model, it was considered that an individual GBS mechanism was operative during the third stage (ε = 0.4–0.7) so, for this stage it is proposed that the Dorn equation can describe this mechanism, but with values of the parameters n, p and Q that correspond to each deformation value. These values, which were determined in Sect. 3.3, showed a decrease that reflected the transition between GBS mechanism and microstructural accommodation for a CGBS mechanism. For true strains values greater than 0.7, the presence of plastic instability made it difficult to determine the parameters to define an equation that appropriately described the deformation mechanism.

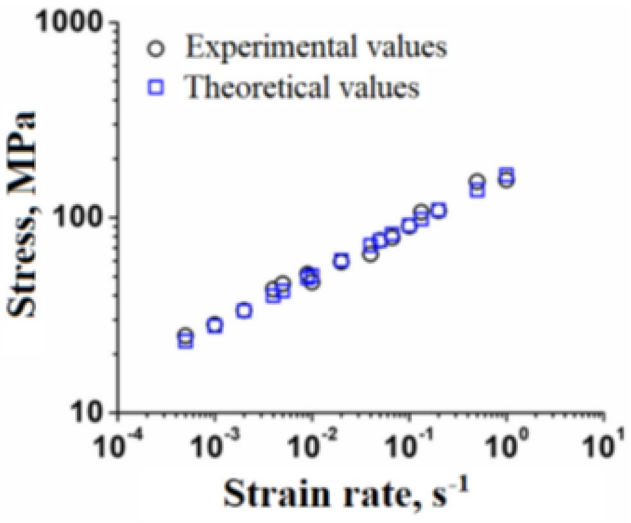

Fig. 16 Graph of the σ vs. strain rate for Zn-21Al-2Cu alloy deformed at 513 K. A strong correlation is observed between values obtained experimentally and those calculated using Eq. 4

5 Conclusions

In this work, we studied the microstructural changes that occur under different conditions of superplastic deformation of the Zn-21Al-2Cu alloy in tension. The aim was to propose a phenomenological model that allows us to determine the conditions under which greater deformation is achieved. The main conclusions are listed below:

1. The results of microstructural changes and mechanical response, including the study of plastic stability, allowed us to propose a phenomenological model of dynamic superplasticity in Zn-21Al-2Cu alloy that consists of five stages as a function of true strain.
2. In the first stage, up to true strain of 0.2 there was a movement of the fine grains that disrupted coherence, increasing misorientation angles between grains to facilitate plastic flow in a steady state regime.
3. Steady flow, operating up to a true strain of approximately 0.4 occurred through an individual GBS mechanism assisted by different micro-mechanisms. These include grain growth, movement of grains from the inner to the surface, migration of grain boundaries and movement of FβBs.
4. For true strains between 0.4 and 0.7, it was found a transition stage where the GBS is partially hindered by the movement and tendency to alignment of FβBs. This transition caused the onset of plastic instability.
5. For a true strain between 0.7 and 1.5, a cooperative grain boundary sliding (CGBS) mechanism was observed to compete with individual GBS, resulting in an increase in plastic instability. At this stage a dynamic growth of grains assisted by deformation is observed.
6. In the last stage, the alignment of FβBs parallel to the tensile direction favored the individual GBS again. Furthermore, the operation of a diffusion flow mechanism was observed, particularly for the Zn-rich η phase. This mechanism led to formation of flow bands which were observed on surface of the highly deformed sample.
7. In a steady state the superplastic mechanism of the Zn-21Al-2Cu alloy can be described by the constitutive equation of plastic flow at high temperature. However depending on the strain, the constitutive equation should be adjusted with specific values of n, p and Q.

Acknowledgements Authors of this work are grateful for the facilities provided by the CCIM-UASLP, the Instituto de Investigación de Materiales at the UNAM and Instituto de Metalurgia of the UASLP. These facilities enable us to carry out the experimental work within the collaboration agreement between both Institutions. We also extended our gratitude to Dr. Jesús Negrete Sánchez for his collaboration in the discussion of these results, and to María Guadalupe Rodríguez, Minerva Aranda, Margarita Álvarez and Alfredo Ruiz for their technical assistance.

Declarations

Conflict of Interest On behalf of all authors, the corresponding author states that there is no conflict of interest.

References

1. T.G. Langdon, J. Mater. Sci. **44**, 5998 (2009)
2. M. Kawasaki, T.G. Langdon, J. Mater. Sci. **42**, 1782 (2007)
3. T.G. Langdon, Mech. Mater. **67**, 2 (2013)
4. M. Kawasaki, T.G. Langdon, Mater. Sci. Eng. A **503**, 48 (2009)
5. P. Kumar, C. Xu, T.G. Langdon, Mater. Sci. Eng. A **429**, 324 (2006)
6. U. Tokuteru, T. Yorinobu, M. Kawasaki, K. Higashi, Lett. Mater. **5**, 269 (2015)
7. M.E. Cetin, M. Demirtas, H. Sofuoglu, Ö.N. Cora, G. Purcek, Mater. Sci. Eng. A **672**, 78 (2016)
8. T.G. Langdon, Mater. Sci. Eng. A **174**, 225 (1994)
9. Z.-R. Lin, A.H. Chokshi, T.G. Langdon, J. Mater. Sci. **23**, 2712 (1988)
10. F.A. Mohamed, T.G. Langdon, Acta Metall. **29**, 911 (1981)
11. T.G. Langdon, Acta Mater. **42**, 2437 (1994)
12. T. Kokubo, G. Itoh, Y. Motohashi, Mater. Sci. Forum. **551**, 153 (2007)
13. M. Ramos Azpeitia, E.E. Martínez, G. Flores, Torres-Villaseñor, J. Mater. Sci. **47**, 6206 (2012)
14. M. Ramos-Azpeitia, E. Elizabeth Martínez-Flores, J.L. Hernandez-Rivera, G. Torres-Villaseñor, J. Mater. Eng. Perform. **26**, 5304 (2017)
15. M. Ramos Azpeitia, E.E. Martínez Flores, J.L. Hernandez Rivera, G. Torres, Villaseñor, J. Mater. Res. Technol. **9**, 5610 (2020)
16. T.G. Langdon, J. Mater. Sci. **41**, 597 (2006)
17. Z. Shi, Y. Ye, S. Li, X. Teng, H. Wang, Chin. Sci. Bull. **47**, 1228 (2002)
18. A. Arieli, A.K. Mukherjee, Metall. Mater. Trans. Phys. Metall. Mater. Sci. **13**, 717 (1982)
19. M.G. Zelin, Mater. Charact. **37**, 311 (1996)
20. E. Sato, K. Kuribayashi, ISIJ Int. **33**, 825 (1993)
21. A.H. Chokshi, Scr. Mater. **44**, 2611 (2001)
22. D.H. Shin, Y.J. Joo, C.S. Lee, K.-T.T. Park, Scr. Mater. **41**, 269 (1999)
23. N. Du, Y. Qi, P.E. Krajewski, A.F. Bower, Metall. Mater. Trans. Phys. Metall. Mater. Sci. **42**, 651 (2011)
24. A.-B. Ma, Y. Nishida, N. Saito, I. Shigematsu, S.-W. Lim, Mater. Sci. Technol. **19**, 1642 (2003)
25. D.H. Shin, C.S. Lee, W.-J. Kim, Acta Mater. **45**, 5195 (1997)
26. J.J. Blandin, R. Dendievel, Acta Mater. **48**, 1541 (2000)
27. A. Sandoval-Jiménez, J. Negrete, G. Torres-Villaseñor, Mater. Charact. **61**, 1286 (2010)
28. M. Ramos, E.E. Martinez, J.L. Hernandez, G. Torres-Villaseñor, Acta Microsc. **27**, 23 (2018)
29. A. Yousefiani, F.A. Mohamed, Metall. Mater. Trans. Phys. Metall. Mater. Sci. **31**, 163 (2000)
30. M. Kawasaki, T.G. Langdon, Mater. Trans. **49**, 84 (2008)
31. Y. Xun, F.A. Mohamed, Acta Mater. **52**, 4401 (2004)
32. D.S. Wilkinson, C.H. Cáceres, Acta Metall. **32**, 1335 (1984)
33. C.H. Hamilton, Metall. Trans. A **20**, 2783 (1989)
34. C.H. Caceres, D.S. Wilkinson, Acta Metall. **32**, 415 (1984)
35. M. Kh, V.G. Rabinovich, Trifonov, Acta Mater. **44**, 2073 (1996)
36. M.K. Rao, A.K. Mukherjee, J. Mater. Sci. **22**, 459 (1987)
37. J.D. Muñoz-Andrade, M. Aguilar-Sánchez, J. Phys: Conf. Ser. **1221**, 012019 (2019)
38. Y. Motohashi, T. Shibata, J. Jpn Inst. Light Met. **31**, 469 (1981)
39. O.A. Kaibyshev, S.N. Faizova, A.F. Hairullina, Acta Mater. **48**, 2093 (2000)
40. B.P. Kashyap, A. Arieli, A.K. Mukherjee, J. Mater. Sci. **20**, 2661 (1985)
41. O.A. Yakovtseva, A.V. Mikhaylovskaya, V.S. Levchenko, A.V. Irzhak, V.K. Portnoy, Phys. Met. Metallogr. **116**, 908 (2015)
42. M. Ramos Azpeitia, E.E. Martínez Flores, J. Negrete Sánchez, G. Torres, Villaseñor, MRS Online Proceedings Library, 1242, (2010)
43. S. Lv, C. Jia, X. He, Z. Wan, X. Li, X. Qu, Materials **12**, 3667 (2019)
44. M. Zelin, A.K. Mukherjee, K Mater. Sci. Forum. **447**, 41 (2004)
45. V.V. Astanin, S.N. Faizova, K.A. Padmanabhan, Mater. Sci. Technol. **12**, 489 (1996)
46. T. Dursun, C. Soutis, Mater. Des. **56**, 862 (2014)